Geomechanics and Engineering, *Vol. 36, No. 3 (2024) 295-301*
https://doi.org/10.12989/gae.2024.36.3.295

Study on small resistance regions in post-liquefaction shear deformation based on soil's compressive properties

Jongkwan Kim[1a], Jin-Tae Han[1b] and Mintaek Yoo*[2]

[1]*Department of Geotechnical Engineering Research, Korea Institute of Civil Engineering and Building Technology, 283 Goyang-daero, Ilsan-seogu, Goyang-si, 10223, Republic of Korea*
[2]*Department of Civil & Environmental Eng., Gachon University, 1342 Seongnam-daero, Seongnam-si 13120, Republic of Korea*

(*Received October 6, 2023, Revised January 4, 2024, Accepted January 14, 2024*)

Abstract. Understanding the post-liquefaction shear behavior is crucial for predicting and assessing the damage, such as lateral flow, caused by liquefaction. Most studies have focused on the behavior until liquefaction occurs. In this study, we performed undrained multi-stage tests on clean sand, sand-silt mixtures, and silty soils to investigate post-liquefaction shear strain based on soil compressibility. The results confirmed that it is necessary to consider the soil compressibility and the shape of soil particles to understand the post-liquefaction shear strain characteristics. Based on this, an index reflecting soil compressibility and particle shape was derived, and the results showed a high correlation with post-liquefaction small resistance characteristic regardless of soil type and fine particle content.

Keywords: compressibility; density index; lateral spreading; liquefaction; shear strain

1. Introduction

The occurrence of liquefaction induces ground deformation. Post-liquefaction deformation takes the form of settlement, lateral spreading, or a combination of both. In particular, lateral spreading causes more damage than post-liquefaction settlement. Most of the research on liquefaction have mainly focused on the undrained behavior of soil under cyclic loading that leads to liquefaction (Kamata *et al.* 2009, Mohamad and Dobry 1986, Iwasaki 1986, El *et al.* 2016, Dash and Sitharam 2011, Kim and Park 2008, Sonmezer *et al.* 2020, Sonmerzer *et al.* 2022). However, after the 1995 Hyogoken Nanbu earthquake, a concept of performance-based design was developed, based on the awareness of the limitation of the conventional design method, which in turn was based on the safety factor. Although a method to evaluate the post-liquefaction shear strain is necessary for performance-based design, comprehensive attempts have not been made to understand the post-liquefaction shear strain characteristics.

Recently, some research has been conducted on post-liquefaction shear strain. Yasuda *et al.* (1995) and Yasuda *et al.* (1999) applied a monotonic shear loading to a liquefied specimen and confirmed two regions of post-liquefaction shear behavior. One is a region where no shear stress is recovered with shearing because of the small rigidity of soil, and the other is a rigidity recovery region where the shear stress of soil is recovered with shear loading. Their result was consistent with the findings of Vaid and Thomas (1995) (Fig. 1). Thomas (1992) classified the shear behavior after liquefaction into three regions. The first is the region of zero effective stress immediately after liquefaction, indicating zero shear stiffness. The second region is where the shear stiffness gradually recovers with shear deformation, and the third region is where the stress-strain curve is linear, indicating constant shear stiffness.

Shamoto *et al.* (1997) conducted torsional shear tests to examine the post-liquefaction deformation characteristics. They showed that shear strain is composed of two components, i.e., one depending on the change in effective stress and other independent of effective stress. Based on their previous research, Shamoto *et al.* (1998) developed a unified methodology and related chart to evaluate the ground deformation.

The sample's relative density and initial confining pressure can influence the shear behavior after liquefaction. Sitharam *et al.* (2009) evaluated the effect of relative density and initial confining pressure on Ahmedabad sand (India) using cyclic triaxial test equipment, and Shamoto *et al.* (1997), Hyodo *et al.* (1998), and Kokusho *et al.* (2004) performed similar experiments. Their results showed that the relative density of the sample had a significant effect on the shear behavior after liquefaction and the initial confining pressure did not have a considerable impact.

In previous experiments, the soil samples were liquefied by cyclic loading and then analyzed for post-liquefaction behavior by applying undrained monotonic loading. As mentioned earlier, many studies show how the sample condition affects the shear behavior after liquefaction. However, the problem is when performing multi-stage tests with cyclic and monotonic loadings, there is no

*Corresponding author, Assistant Professor
E-mail: mintaekyoo@gachon.ac.kr
[a]Senior Researcher (Ph.D.)
[b]Research Fellow (Ph.D.)

ISSN: 2005-307X (Print), 2092-6219 (Online)

Table 1 Physical properties of soils

Soil type	Specific gravity G_s	Maximum void ratio e_{max}	Minimum void ratio e_{min}	Fines content F_c (%)
Iide silica sand #7	2.69	1.015	0.626	0
Gifu silica sand #7	2.65	1.226	0.720	0
Iwaki silica sand #6	2.64	1.303	0.826	0
DL Clay	2.67	1.65	0.82	97
Quartz powder	2.74	2.35	1.17	90
Aratosawa silty soil	2.42	2.57	1.51	90
Urayasu silty soil	2.63	1.64	0.88	54

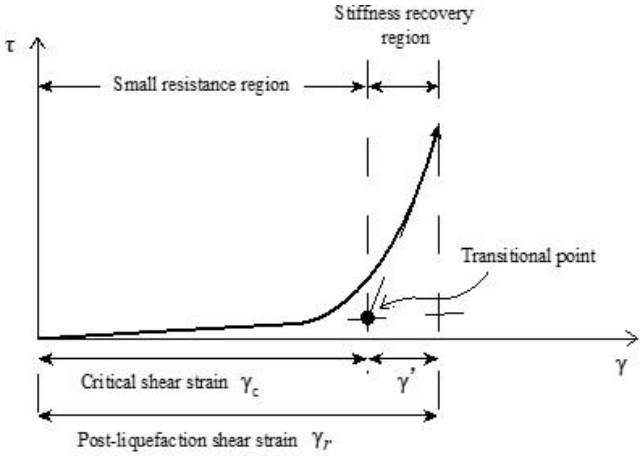

Fig. 1 General post-liquefaction stress-strain behavior (Vaid and Thomas 1995 and Yasuda *et al.*1999)

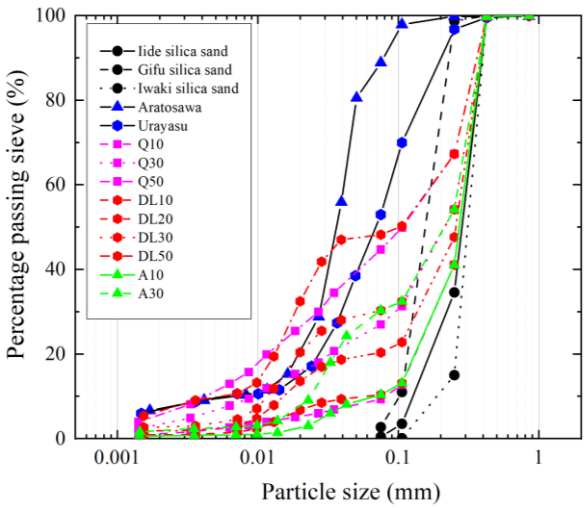

Fig. 2 Particle size distribution of soils

consideration of the loading history during cyclic loading that is applied until liquefaction occurs. According to Ishihara and Yoshimine (1992) and Sento *et al.* (2004), the volume strain after liquefaction is greatly affected by the load history of cyclic loading. Ishihara and Yoshimine (1992) found that the maximum shear strain developed during cyclic loading under constant stress affects the volume deformation after liquefaction.

In addition, Sento *et al.* (2004) reported that the volume strain after liquefaction is more affected by the accumulated shear strain than the maximum shear strain through strain-controlled cyclic loading tests. Therefore, to evaluate the shear behavior after liquefaction, it is necessary to consider the loading history during cyclic loading. In addition, the aforementioned studies on post-liquidation shear behavior focused on identifying regions with different characteristics of post-liquidation shear behavior and estimating the shear stiffness of each region. However, from the perspective of performance design, it is necessary to review not only the shear stiffness after liquefaction but also how long the region with zero shear stiffness, commonly referred to as region 1, continues.

In this study, a multi-stage test set that combines cyclic loading and monotonic loading has been performed. The post-liquefaction shear behavior was analyzed, mainly focused on small resistance regions. Test results were examined based on the soil compressibility..

2. Methodology

2.1 Soils properties

We used clean sand, artificial sand-silt mixtures, and natural silty soils for the test. Iide silica sand #7, Gifu silica sand #7, and Iwaki silica sand #6 were prepared as clean sand. Sand-silt mixtures were prepared by mixing Iide silica (disturbed), were sampled in situ where liquefaction occurrence was observed during the Iwate-Miyagi Nairiku earthquake in 2008 and 2011 off the Pacific coast of Tohoku earthquake(Kazama *et al.* 2019; Yamaguchi *et al.* 2012) were also prepared for the test. Table 1 and Fig. 2 illustrate soil samples' properties and particle size distribution. All soils used in this study are non-plastic.

2.2 Density index

The soil density has a significant impact on its dynamic behaviour as well as its shear deformation properties after liquefaction. Since this study deals with fine-grained soils and clean sands, the choice of density index is essential, as the most widely used relative density is not applicable when the fines are more significant than 5% Japanese Geotechnical Society or 15% American Society for Testing and Materials. In previous studies, the authors pointed out this limitation(Kim *et al.* 2019). They proposed a new

Table 2 Test cases

No	ID	FC	e[1]	CSR[2]	Dr(%)	$e_{min.c}$[3]	$\varepsilon_{v,u}$[4]	Remark
1	I7	0	0.863	0.4	32.8	0.566	0.162	Iide silica sand
2	I7	0	0.824	0.2	42.6		0.141	
3	I7	0	0.801	0.4	48.8		0.128	
4	I7	0	0.796	0.2	56.6		0.111	
5	I7	0	0.796	0.2	64.4		0.093	
6	I7	0	0.795	0.2	33.8		0.160	
7	I7	0	0.761	0.2	47.6		0.131	
8	I7	0	0.715	0.4	66.7		0.087	
9	G7	0	1.010	0.1	42.7	0.669	0.169	Gifu silica sand
10	G7	0	1.010	0.15	42.6		0.170	
11	G7	0	0.984	0.13	47.8		0.159	
12	G7	0	0.903	0.2	85.2		0.069	
13	G7	0	0.794	0.3	85.4		0.070	
14	G7	0	0.795	0.25	84.7		0.071	
15	G7	0	0.798	0.33	63.8		0.123	
16	Iwa6	0	1.089	0.2	44.9	0.756	0.159	Iwaki sand
17	Iwa6	0	1.082	0.25	46.3		0.157	
18	Iwa6	0	1.061	0.22	50.7		0.148	
19	Iwa6	0	1.025	0.3	58.3		0.133	
20	Iwa6	0	0.911	0.3	82.2		0.081	
21	U	54	1.063	0.2	58.2	0.649	0.201	Urayasu silty soil
22	U	54	0.935	0.2	71.1		0.148	
23	U	54	0.877	0.2	76.9		0.122	
24	Ara	90	1.893	0.2	49.9	1.214	0.235	Aratosawa silty soil
25	Ara	90	1.550	0.2	75.2		0.132	
26	Q10	10	0.655	0.4	63.5	0.449	0.125	Quartz power 10%
27	Q10	10	0.738	0.2	48.9		0.167	
28	Q30	30	0.728	0.2	51.8	0.287	0.255	Quartz power 30%
29	Q30	30	0.556	0.2	70.6		0.173	
30	Q50	50	0.65	0.2	80.7	0.449	0.124	Quartz power 50%
31	DL10	10	0.744	0.2	38.1	0.423	0.184	DL Clay 10%
32	DL10	10	0.664	0.2	53.5		0.145	
33	DL10	10	0.589	0.4	68.0		0.105	
34	DL20	20	0.617	0.2	47.9	0.328	0.179	DL Clay 20%
35	DL30	30	0.602	0.2	46.8	0.264	0.211	DL Clay 30%
36	DL30	30	0.464	0.2	68.6		0.137	
37	DL50	50	0.625	0.2	59.1	0.346	0.172	DL Clay 50%
38	DL50	50	0.565	0.2	67.9		0.140	
39	DL50	50	0.494	0.2	78.3		0.099	
40	A10	10	0.759	0.2	50.6	0.499	0.148	Aratosawa 10%
41	A30	30	0.856	0.2	54.4	0.533	0.174	Aratosawa 30%

[1] e = initial void ratio
[2] CSR = Cyclic stress ratio
[3] $e_{min.c}$ = Cyclic minimum void ratio
[4] $\varepsilon_{v,u}$ = Ultimate volumetric strain

density index called ultimate volumetric strain based on the compressive properties of soil. They showed that this density index expresses the volumetric deformation characteristics after liquefaction well, regardless of soil type (Kim *et al.* 2019, Kim *et al.* 2021). Therefore, the ultimate volumetric strain was used to evaluate the post-liquefaction shear properties in this study.

The ultimate volumetric strain is the volumetric strain potential of soil in a given state when liquefied and drained to infinity. Therefore, a considerable ultimate volumetric strain means that the amount of volumetric strain that can occur after liquefaction is large. According to Oshima *et al.* (2008) and Shamoto *et al.* (1998), there is a correlation between the volumetric strain and shear strain after liquefaction. Therefore, it can be assumed that the volume strain after liquefaction is significant, and the shear strain after liquefaction is also large. The ultimate volumetric strain is defined as

$$\varepsilon_{v,u} = \frac{e_0 - e_{min.c}}{1 + e_0} \quad (1)$$

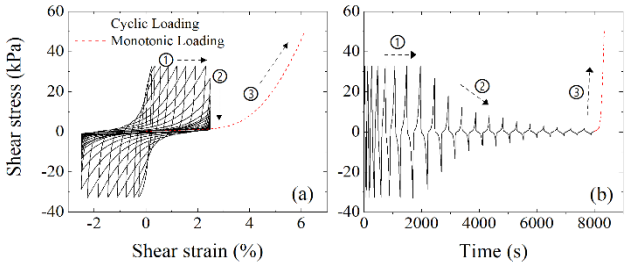

Fig. 3 Example of the test procedure ((a) stress-strain loop and (b) time history of shear stress)

where e_0 is the initial void ratio and $e_{min.c}$ is a cyclic minimum void ratio that is finally obtained by repeating liquefaction and drainage repeatedly (Kim *et al.* 2019). The initial void ratio and cyclic minimum void ratio of each soil sample are shown in Table 2. The ultimate volumetric strain can be calculated based on the N1 value by referring to the previous research (Kim *et al.* 2021, Numata *et al.* 2002, Ishihara *et al.* 2016).

2.3 Test apparatus and loading procedure

The hollow cylindrical torsional shear test apparatus was utilized for the test. Samples with an outer diameter of 7 cm, an inner diameter of 3 cm, and a height of 10 cm were saturated with carbon dioxide and de-aired water, and all specimens had a B-value greater than 0.95. All saturated specimens were consolidated with 100 kPa irrespective of soil type. We conducted a multi-stage experiment consisting of cyclic and monotonic loading as proposed by the authors in their previous work (Kim *et al*. 2017). Cyclic loading consists of constant stress amplitude cyclic loading(1 in Fig. 3) and constant strain amplitude cyclic loading(2), followed by monotonic loading(3). During the constant stress amplitude cyclic loading, when the shear strain of the specimen reaches single amplitude of 2.5%, switch to constant strain amplitude cyclic loading and continue loading until the stress-strain loop is converged. This creates a state of the apparent lower stiffness limit where the stiffness is sufficiently reduced without inducing a large deformation. So, it is possible to compare the post-liquefaction shear strain development potential at an apparent lower stiffness limit irrespective of loading history. Fig. 3 shows an example of a test procedure.

3. Test results

Figs. 4 and 5 show a post-liquefaction shear behaviour at similar relative density and ultimate volumetric strain, respectively. In Fig. 4, I7 and DL10 show similar shear behaviour after liquefaction, but when the sample type and fines content vary, no clear correlation can be found, even at the same relative density. The characteristic is that the recovery of shear stiffness after liquefaction is slower as the fines content increases at the same relative density. Ultimate volumetric strain also showed no clear trend (Fig. 5).

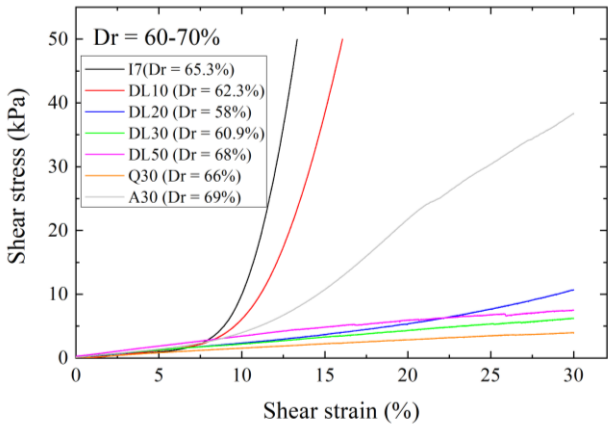

Fig. 4 Shear stress-strain curve after cyclic loading (relative density)

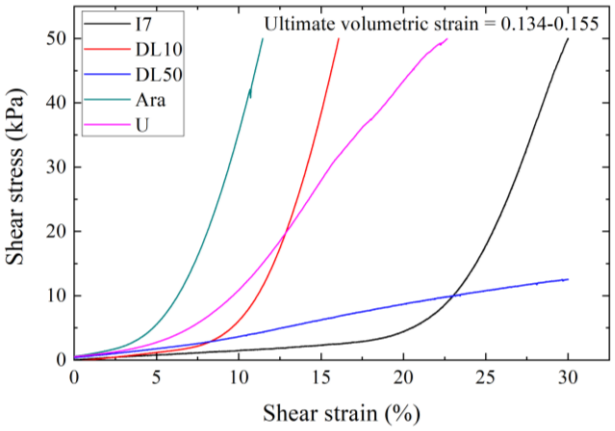

Fig. 5 Shear stress-strain curve after cyclic loading (ultimate volumetric strain)

However, Fig. 5 shows that the time when shear stiffness starts to recover is different, still, the trend after stiffness recovery is similar except for Urayasu and DL50. It is believed that the stiffness recovery behavior of Urayasu and DL50 is different due to the higher fines content compared to other samples. Therefore, post-liquefaction shear behavior was classified into a small resistance region and stiffness recovery region, as shown in Fig. 1. However, the conventional method uses the point where the tangent lines of the two regions meet as the transition point, as shown in Fig. 1. However, in the case of soil containing a lot of fine particles as shown in Fig. 4 (DL20, DL30, DL50 and Q30), it is impossible to identify the transition point because there is no change in the slope until the shear strain reaches 30%. Fig. 6 shows the effective stress path under monotonic loading after liquefaction.

From the results of the effective stress near 0, it can be seen that the effective stress and shear stress increase with monotonic loading, and the slope becomes constant when the effective stress is more significant than about 1 kPa. Since the continuous increase in the slope can be considered as the recovery of shear stiffness, the time until the effective stress is recovered by 1 kPa is judged as a small resistance region, and the amount of shear strain at this time is defined

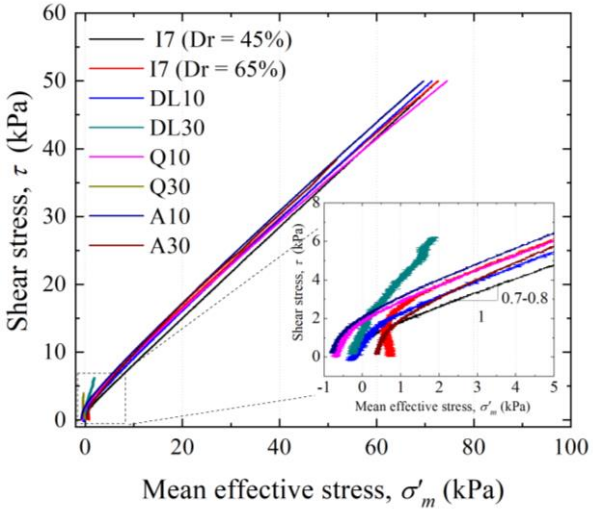

Fig. 6 Effective stress path during post-liquefaction monotonic loading

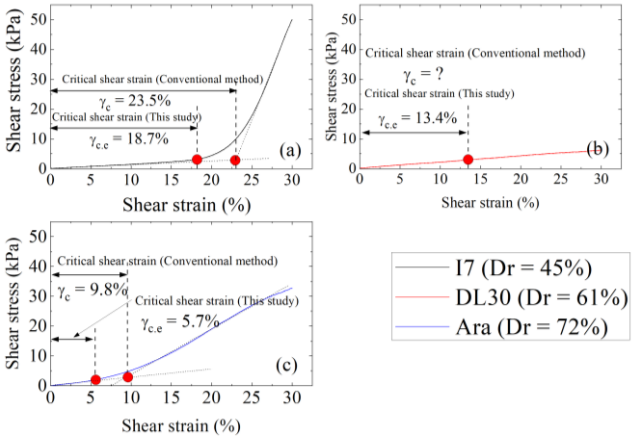

Fig. 7 Difference between the critical shear strains obtained based on the conventional method and effective stress

as the critical shear strain, $\gamma_{c.e}$. Fig. 7 shows the comparison results of the existing and newly proposed methods in this study. It can be seen that the critical shear strain estimated based on the recovery of the effective stress is smaller than that estimated by the conventional method(Fig. 1) and coincides with the time when the angle of the shear strain-stress curve starts to change. In addition, the effective stress method can determine the critical shear strain even when the transitional point is unclear, as shown in Fig. 7(b).

In Fig. 7(a), the post-liquefaction shear deformation is divided into two regions as shown in Fig. 1. In the small resistance region, the amount of deformation is constant regardless of the boundary conditions, and then the deformation in the stiffness recovery region depends on the boundary conditions. For example, in the case of sloping ground or the bottom of an embankment, the amount of shear stress that is required to stop the deformation is different depending on such as location or inclination. Therefore, this study focuses on the amount of deformation in the small resistance region that developed regardless of the boundary condition.

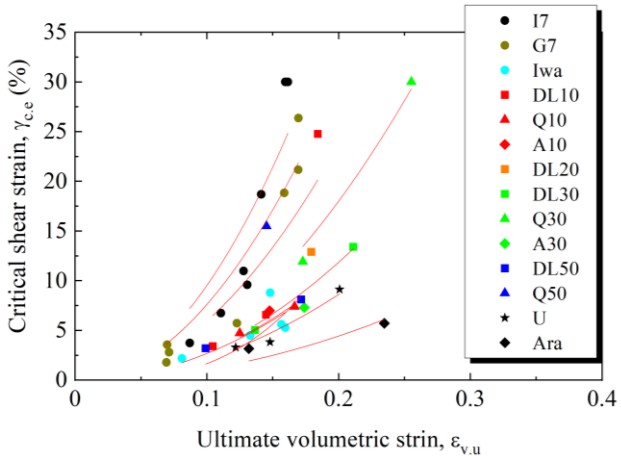

Fig. 8 Relationship between critical shear strain and ultimate volumetric strain

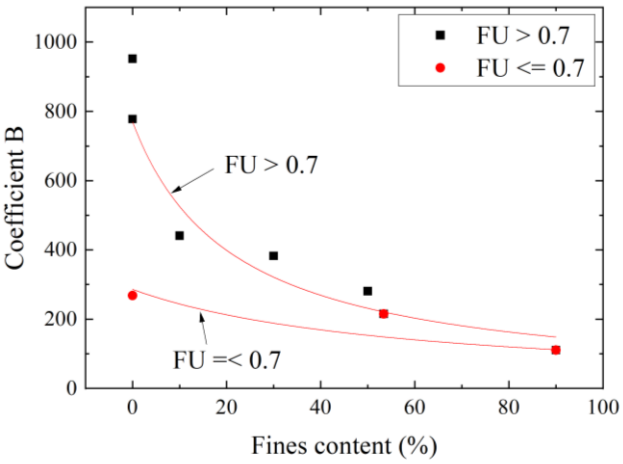

Fig. 9 Variation in coefficient B with fines content and FU

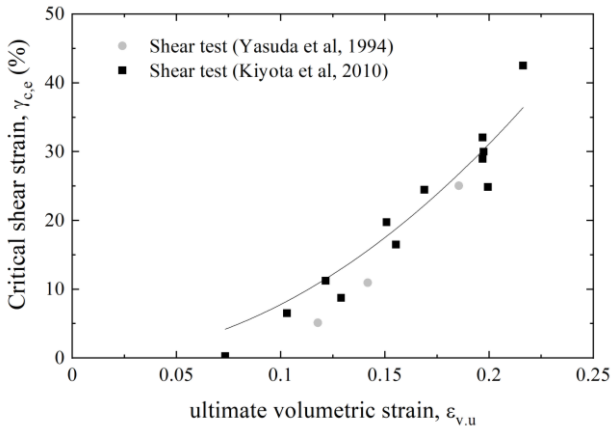

Fig. 10 Critical shear strain against ultimate volumetric strain (Toyoura sand)

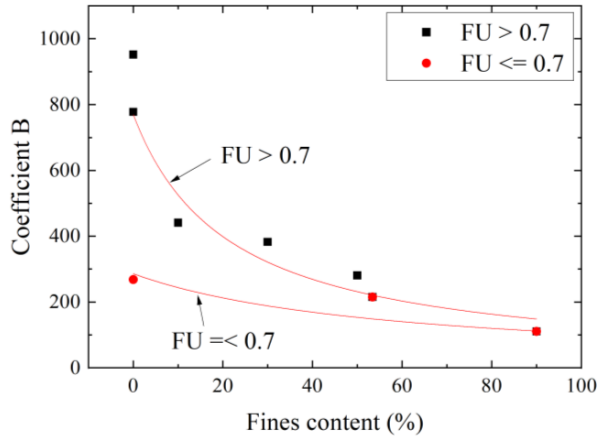

Fig. 11 Critical shear strain against the modified ultimate volumetric strain of Toyoura sand

Fig. 8 shows the relationship between ultimate volumetric strain and critical shear strain. It can be seen that for the same ultimate volumetric strain, the critical shear strain is different for different soil types. This means that the ultimate volumetric strain cannot represent the critical shear strain. The regression lines in Fig. 8 show the results of fitting $y = Bx^2$ for each soil type. The results show that the regression line moves to the lower right as the fines content increases. However, in the case of Iwaki sand, despite being a clean sand, the trend is similar to that of soils with high fines content. Unlike Iide silica sand and Gifu silica sand, Iwaki sand is characterized by a very angular grain shape, and it can be assumed that the grain shape affects the critical shear strain (Kim *et al.* 2019, Li *et al.* 2013). Fig. 9 summarizes coefficient B based on the fine contents and coefficient of form unevenness (Yoshimura and Ogawa 1993). Here, the coefficient of form unevenness (FU) indicates the particle's shape and shows a value between 0 and 1, where 1 means round. Coefficient B becomes smaller as the fines content increases, and it can be seen that it has a different trend based on FU 0.7. Based on the results in Fig. 9, the coefficient B can be calculated from the following equation.

$$B = \frac{1}{b + 6 \cdot 10^{-5} \times FC(\%)}, \tag{2}$$

where b is the coefficient relating to the particle shape. 0.0013 and 0.0035 were adopted for coefficient b when FU is larger and smaller than 0.7, respectively. Thus, the critical shear strain can be estimated by

$$\gamma_{c.e} = B \cdot (\varepsilon_{v,u})^2 \tag{3}$$

Eqs. (2) and (3) can be used to calculate the critical shear strain, but there is still an effect of soil particle shape. To eliminate the effect of soil particle shape, normalization was performed based on the particle shape of Toyoura sand, and the ultimate volumetric strain was modified based on this. Fig. 10 is the result of summarizing the critical shear strain of Toyoura sand derived from the studies of Yasuda *et al.* (1994) and Kiyota *et al.* (2010) concerning the ultimate volumetric strain and the B-value of Toyoura sand (B_T) was 777. Based on this result, the modified ultimate volumetric strain can be calculated as follows.

$$\varepsilon^*_{v.u} = \sqrt{\frac{B}{B_T}} \cdot \frac{e_0 - e_{min.c}}{1 + e_0} \tag{4}$$

The results of summarizing the critical shear strain based on the modified ultimate volumetric strain are shown in Fig. 11. In Fig. 11, not only the experimental results of this study, but also the laboratory shear test results and model test results for Toyoura sand are shown. From the results, it can be seen that the experimental results of this study and previous studies are in good agreement. It can be seen that the critical shear strain can be predicted fairly well based on a single index calculated based on particle shape and compressive properties, despite the fact that this study used clean sand and also samples with various types of fines and various contents.

The ultimate volumetric strain can be calculated based on the N1 value by referring to the previous researches(Kim *et al.* 2021, Numata *et al*. 2002, Ishihara *et al.* 2016). Kim *et al.* (2021) suggested a chart to obtain the cyclic minimum void ratio based on the minimum void ratio. Minimum void ratio of in-situ can be calcuated using a procedure which estimates the maximum and minimum void ratio based on SPT-N value. Precise equations and procedure can be found from the references.

4. Conclusions

This study investigated post-liquefaction shear deformation characteristics using multi-stage loading tests on three types of clean sands: sand-silt mixtures with varying fines content and two in situ silty soils. To exclude the effect of reloading force, the unloading method of constant stress amplitude cyclic loading and constant strain amplitude cyclic loading was used to bring each sieve to the apparent lower stiffness limit. After cyclic loading, the post-liquefaction shear deformation characteristics were determined using undrained monotonic loading based on the relative density and ultimate volumetric strain, representing the soil's compressive properties. The results showed that even for the same relative density, different soil types and fine content showed varying trends. Ultimate volumetric strain also did not show a clear correlation with post-liquefaction small resistance region. It can be seen that it is difficult to evaluate post-liquefaction shear strain based on volume deformation properties alone. For detailed analysis, the post-liquefaction shear strain was divided into a small resistance region and a stiffness recovery region, and the analysis was focused on the small resistance region. This study proposed a method to define the small resistance region as the moment the effective stress reaches 1 kPa during post-liquefaction monotonic loading. As a result, it tends to be evaluated smaller than the existing tangent line estimation method.

The critical shear strain, which represents the amount of small resistance region, did not show a clear correlation with the ultimate volumetric strain. Still, when the coefficient of FU, which represents the shape of soil particles, was introduced and examined, it was found to be affected not only by the compressive properties of the soil but also by the shape of the soil particles.

Therefore, we derived a modified ultimate volumetric strain that considers the effect of soil particles, and the experimental results showed a good agreement with that of previous studies. However, the problem is the FU, which represents the particle shape, and further research is needed on how to estimate the FU for practical estimation.

Acknowledgments

Research for this paper was carried out under the KICT esearch Program (Database construction for ground liquefaction assessment based on AI technology, 2024) funded by the Ministry of Science and ICT.

References

Dash, H.K. and Sitharam, T.G. (2011), "Cyclic liquefaction and pore pressure response of sand-silt mixtures", *Geomech. Eng.*, **3**(2), 83-108. https://doi.org/10.12989/gae.2011.3.2.083.

El Takch, A., Sadrekarimi, A. and El Naggar, H. (2016), "Cyclic resistance and liquefaction behavior of silt and sandy silt soils", *Soil Dyn. Earthq. Eng.*, **83**, 98-109. https://doi.org/10.1016/j.soildyn.2016.01.004.

Hamada, M., Sato, H. and Kawakami, T. (1994), "A consideration of the mechanism for liquefaction-related large ground displacement", *Proceedings of the 5th US-Japan Workshop on Earthquake Resistant Design of Lifeline Facilities and Countermeasures against Soil Liquefaction*.

Hyodo, M., Hyde, A.F.L. and Aramaki, N. (1998), "Liquefaction of crushable soils", *Geotechnique*, **48**(4), 527-543. https://doi.org/10.1680/geot.1998.48.4.527.

Ishihara, K., Harada, K., Lee, W.F., Chan, C.C. and Safiullah, A.M.M. (2016), "Post-liquefaction settlement analyses based on the volume change characteristics of undisturbed and reconstituted samples", *Soils Found.*, **56**(3), 533-546. https://doi.org/10.1016/j.sandf.2016.04.019.

Iwasaki, T. (1986), "Soil liquefaction studies in Japan: state-of-the-art", *Soil Dyn. Earthq. Eng.*, **5**(1), 2-68. https://doi.org/10.1016/0267-7261(86)90024-2.

Kamata, T., Tsukamoto, Y. and Ishihara, K. (2009), "Undrained shear strength of partially saturated sand in triaxial tests", *Bull. N. Z. Soc. Earthq. ng.*, **42**(1), 57-62. https://doi.org/10.5459/bnzsee.42.1.57-62.

Kim, J., Kawai, T. and Kazama, M. (2017), "Laboratory testing procedure to assess post-liquefaction deformation potential", *Soils Found.*, **57**(6), 905-919. https://doi.org/10.1016/j.sandf.2017.10.001.

Kim, J., Kawai, T. and Kazama, M. (2019), "Minimum void ratio characteristic of soils containing non-plastic fines", *Soils Found.*, **59**(6), 1772-1786. https://doi.org/10.1016/j.sandf.2019.08.001.

Kim, J., Kazama, M. and Kawai, T. (2021), "Evaluation of post-liquefaction volumetric strain of reconstituted samples based on soil compressibility", *Soils Found.*, **61**(6), 1555-1564. https://doi.org/10.1016/j.sandf.2021.09.002.

Kim, S. and Park, K. (2008), "Proposal of liquefaction potential assessment procedure using real earthquake loading", *KSCE J. Civ. Eng.*, **12**(1)**,** 15-24. https://doi.org/10.1007/s12205-008-8015-9.

Kiyota, T., Koseki, J. and Sato, T. (2010), "Comparison of liquefaction-induced ground deformation between results from undrained cyclic torsional shear tests and observations from previous model tests and case studies", *Soils Found.*, **50**(3), 421-429. https://doi.org/10.3208/sandf.50.421.

Kokusho, T., Hara, T. and Hiraoka, R. (2004), "Undrained shear

strength of granular soils with different particle gradation", *J. Geotech. Geoenviron. Eng.*, **130**(6), 621-629. https://doi.org/10.1061/(ASCE)1090-0241(2004)130:6(621).

Li, Y., Huang, R., Chan, L.S. and Chen, J. (2013), "Effects of particle shape on shear strength of clay-gravel mixture", *KSCE J. Civ. Eng.*, **17**(4)**,** 712-717. https://doi.org/10.1007/s12205-013-0003-z.

Mohamad, R. and Dobry, R. (1986), "Undrained monotonic and cyclic triaxial strength of sand", *J. Geotech. Eng*., **112**(10), 941-958. https://doi.org/10.1061/(ASCE)0733-9410(1986)112:10(941).

Numata, A., Someya, N., Tazoh, T. and Kokusho, T. (2002), "Proposal of definition of minimum void ratio for fine soils", *Proceedings of the 11th Japanese Earthquake Engineering Symposium.*

Shamoto, Y., Zhang, J.M. and Goto, S. (1997), "Mechanism of large post-liquefaction deformation in saturated sand", *Soils Found.*, **37**(2), 71-80. https://doi.org/10.3208/sandf.37.2_71.

Shamoto, Y., Zhang, J.M. and Tokimatsu, K. (1998), "Methods for evaluating residual post-liquefaction ground settlement and horizontal displacement", *Soils Found.*, **38**, 69-83. https://doi.org/10.3208/sandf.38.Special_69.

Sitharam, T.G., Vinod, J.S. and Ravishankar, B.V. (2009), "Post-liquefaction undrained monotonic behaviour of sands: experiments and DEM simulations", *Géotechnique*, **59**(9), 739-49. https://doi.org/10.1680/geot.7.00040.

Sonmezer, Y.B., Akyuz, A. and Kayabali, K. (2020), "Investigation of the effect of grain size on liquefaction potential of sands", *Geomech. Eng.*, **20**(3), 243-254. https://doi.org/10.12989/gae.2020.20.3.243.

Sonmezer, Y.B., Kyabali, K., Beyaz, T. and Fener, M. (2022), "Influence of grain size ratio and silt content on the liquefaction potentials of silty sands", *Geomech. Eng.*, **31**(2), 167-181, https://doi.org/10.12989/gae.2022.31.2.167.

Thomas, J. (1992), *Static, Cyclic and Post Liquefaction Undrained Behaviour of Fraser River Sand* [Ph.D. Thesis]. *University of British Columbia.*

Vaid, Y.P. and Thomas, J. (1995), "Liquefaction and postliquefaction behavior of sand", *J. Geotech. Eng*., **121**(2), 163-173. https://doi.org/10.1061/(ASCE)0733-9410(1995)121:2(163).

Yasuda, S., Masuda, T., Yoshida, N., Nagase, H., Kiku, H., Itafuji, S., Mine, K. and Sato, K. (1994), "Torsional shear and triaxial compression tests on deformation characters of sands before and after liquefaction", *Proceedings of the 5th US-Japan Workshop on Earthquake Resistant Design of Lifeline Facilities and Countermeasures against Soil Liquefaction*.

Yasuda, S., Nagase, H., Mine, K., Yoshida, M., Kiku, H. and Masuda, T. (1995), "Stress-strain relationship of liquefied sands", *Proceedings of the 1st International Conference on Earthquake Geotechnical Engineering.*

Yasuda, S., Yoshida, N., Adachi, K., Kiku, H., Gose, S. and Masuda, T. (1999), "A simplified practical method for evaluating liquefaction-induced flow", *Doboku Gakkai Ronbunshu*, **1999**(638), 71-89. https://doi.org/10.2208/jscej.1999.638_71.

Yoshimura, Y. and Ogawa, S. (1993), "A simple quantification method of grain shape of granular materials such as sand", *Doboku Gakkai Ronbunshu*, **1993**(463), 95-103. https://doi.org/10.2208/jscej.1993.463_95.